AIP | Applied Physics Letters

Growth of high-density vertically aligned arrays of carbon nanotubes by plasma-assisted catalyst pretreatment

S. Esconjauregui, B. C. Bayer, M. Fouquet, C. T. Wirth, C. Ducati et al.

Citation: Appl. Phys. Lett. **95**, 173115 (2009); doi: 10.1063/1.3256012
View online: http://dx.doi.org/10.1063/1.3256012
View Table of Contents: http://apl.aip.org/resource/1/APPLAB/v95/i17
Published by the American Institute of Physics.

Growth of high-density vertically aligned arrays of carbon nanotubes by plasma-assisted catalyst pretreatment

S. Esconjauregui,[1,a)] B. C. Bayer,[1] M. Fouquet,[1] C. T. Wirth,[1] C. Ducati,[2] S. Hofmann,[1] and J. Robertson[1]
[1]*Department of Engineering, University of Cambridge, 9 JJ Thomson Avenue, Cambridge CB3 0FA, United Kingdom*
[2]*Department of Materials Science and Metallurgy, University of Cambridge, Cambridge CB3 0FA, United Kingdom*

(Received 21 April 2009; accepted 6 October 2009; published online 30 October 2009)

A plasma-assisted thermal pretreatment of catalyst films (Ni, Co, or Fe) greatly facilitates the direct growth of high-density vertically aligned arrays of small diameter carbon nanotubes (CNTs) on conductive TiN by purely thermal chemical vapor deposition. Purely thermal catalyst pretreatment gives limited or no growth. The plasma-assisted pretreatment promotes a stronger catalyst-support interaction, which reduces catalyst mobility and hence stabilizes smaller catalyst particles with a higher number density. © *2009 American Institute of Physics*. [doi:10.1063/1.3256012]

Carbon nanotubes (CNTs) have many potentially uses in electronics, as interconnects in integrated circuits, field emitters, supercapacitor electrodes, sensors, or thermal management surfaces.[1–6] Many such applications require small diameter nanotubes in the form of densely packed vertically aligned mats on conducting substrates. There are two ways to obtain vertically aligned CNTs (VACNTs). The first is to use plasma enhanced chemical vapor deposition (CVD), in which the electric field of the plasma sheath aligns the nanotubes normal to the surface.[7,8] This method is particularly suitable for growing larger diameter multiwall nanotubes in sparse arrays, suitable for field emission.[8] The second method is to grow densely packed arrays by CVD, where the high packing density itself causes the vertical alignment. In that case, the high density generally arises from a particular catalyst design such as thin Fe catalyst layers on Al_2O_3 support.[2,9–11] The limitation of this method is that these materials are insulators. Direct CVD growth of CNTs on conducting substrates such as TiN is more challenging and does not usually yield high-density mats.[12–16]

A growing CNT is entirely fed by the catalyst particle, so the catalyst particle size dictates the CNT diameter. For surface-bound CVD, the catalyst-support interactions play a crucial role in controlling the catalyst particle size distribution. Physical vapor deposited catalyst films dewet upon annealing, whereby the catalyst transformation is driven by the difference in surface energy of the support layer and the metal catalyst.[17] An oxide support has low surface energy, so this naturally induces dewetting of higher surface energy metals. But if the support is also a high surface energy metal, the catalyst dewets less readily.[14] Generally, unlike inert oxides, a high surface energy metal will strongly interact with the gas atmosphere; hence, a metal-metal catalyst-support system, at the elevated temperatures and reactive atmospheres of CNT CVD, is more difficult to control.

Here, we note that the nucleation density and diameter of nanotubes can be controlled by restructuring the catalyst *prior* to growth, in a separate restructuring step, and separately controlling the restructuring conditions.[18,19] We employ this technique here to establish a method to obtain high density mats of small diameter nanotubes on TiN support.

We first dc magnetron sputter a 100 nm TiN onto a Si wafer coated with 200 nm of thermal SiO_2. We then sputter a nominally 1 nm thick layer of high purity Fe, Co, or Ni onto the TiN layer (after exposing the TiN sample to air). Using a cold-wall plasma chamber (base pressure $\sim 10^{-6}$ mbar), these layers are subjected to either purely thermal pretreatment (TP) or plasma-assisted thermal pre-treatment (PP). TP is performed for 5 min at 450 to 800 °C in 100 mbar of H_2. Alternatively, the catalyst is pretreated at similar range of temperatures, time, and pressure in a 50 W dc plasma. Immediately after either pretreatment, the chamber is evacuated and CNT growth is carried out by purely thermal CVD in undiluted C_2H_2 at ~0.5 mbar for 10 min–1 h. Note that the absence of a direct plasma during growth (as against a remote plasma[5]) is important, as it avoids ion damage to CNTs. TiN support, catalyst and CNT films are examined by a scanning electron microscope (SEM), high resolution transmission electron microscopy (HRTEM), x-ray diffraction (XRD), and atomic force microscope (AFM). Nanoparticle and CNT densities are estimated from SEM and AFM images using both IMAGEJ and GWYDDION software.

After pretreatment, the catalytic films are strongly restructured (Fig. 1). Following TP, the films clearly become discontinuous with a broad distribution of particle sizes, Figs. 1(a) and 1(c). Conversely, all the films following PP show smaller particle sizes and higher number density, Figs. 1(d) and 1(f). AFM analysis shows a regular distribution of few-nanometer nanoparticles with minimal separation or overlap, Fig. 2(a). The TP films have RMS roughness of ~50 nm; whereas the PP films have a smoother and more homogeneous surface topology with ~3 nm rms roughness and a nanoparticle height of only ~5 nm. The original nanoparticles are smaller, as they oxidize when transferred in air. We also analyzed the restructuring of the TiN film under TP or PP. XRD and AFM respectively reveal that TiN remains polycrystalline with no changes in surface roughness (results not shown). For a qualitative comparison, we plotted the lateral size distribution of the catalyst particles from each pre-treatment in Figs. 2(b) and 2(d). Figures 2(b) and 2(c)

a)Electronic mail: cse28@cam.ac.uk.

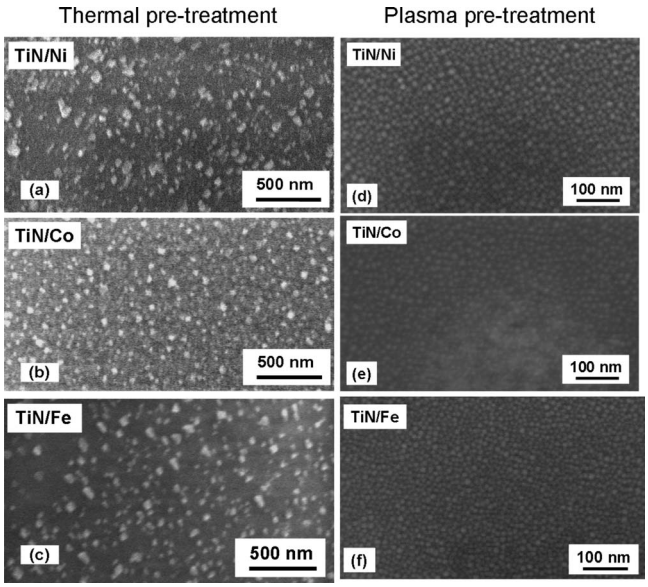

FIG. 1. SEM images of 1 nm Ni, Co, and Fe deposited onto TiN and pretreated for 5 min at 550 °C in 100 mbar of H_2 under [(a)–(c)] TP and [(d)–(f)] PP with a dc plasma power of 50 W.

compare the restructuring of 1 nm Fe film on TiN at 600 °C for 5 min without or with plasma assistance, respectively. These nanoparticles have a narrow lateral size distribution of 9 ± 1 nm for PP, compared to 24 ± 11 nm for TP, Fig. 2(d). The particle density increases from $(1.3 \pm 0.2) \times 10^9$ cm^{-2} for TP to $(8.6 \pm 0.7) \times 10^{11}$ cm^{-2} for PP, as estimated from SEM and AFM images. Ni and Co show a similar behavior.

These different catalyst topographies have a strong effect on the nucleation, growth, and morphology of the resulting CNTs (Fig. 3). Growth is rather poor after TP, Figs. 3(c) and 3(d). These nanoparticles produce entangled CNTs lying laterally and with little alignment, Fig. 3(c). Large nanoparticles hardly show CNT nucleation for our CVD conditions, Fig. 3(d); hence TP only yields low-density partly aligned CNTs, Fig. 5(a) and 5(b).

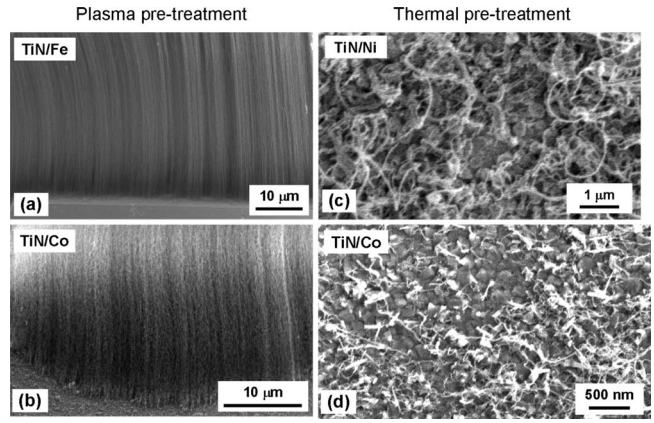

FIG. 3. SEM images of CNTs grown for 10 min in 0.5 mbar of C_2H_2 on (a) Fe and (b) Co films receiving PP; (c) Ni and (d) Co films following TP. For (a), (c), and (d), the growth temperature is 600 °C, but for (b) it is 480 °C.

In contrast, PP leads to growth of high-density VACNTs for all Fe, Co, or Ni catalysts. At 600 °C, we obtained mat densities as high as $\sim 10^{12}$ CNTs/cm^2, as estimated from SEM images, Fig. 3(a). The mats are homogeneous over the sample. The HRTEM image in Fig. 4 indicates that the CNTs are mainly double and triple walled, with diameters under 5 nm. We achieved similar growth down to 480 °C, Fig. 3(b). For all growth conditions, XRD reveals that TiN remains polycrystalline with no phase changes (results not shown).

To assess the CNT growth mode, we exposed PP films to interrupted growth conditions.[6] After PP, C_2H_2 flow is on for 1 min stopped for 5 min; and then on for another 10 min. This creates a two-layer mat with a thicker bottom layer, Fig. 5(c). The thin top layer grew first (1 min growth), followed by the thicker bottom layer (10 min growth). These results confirm base growth.

We find PP to be advantageous for many catalyst-support systems, such as Ni–SiO_2,[19] Fe–Ta, which suggests a generic mechanism. We note the high degree of CNT alignment obtained for PP catalysts. This alignment closely resembles

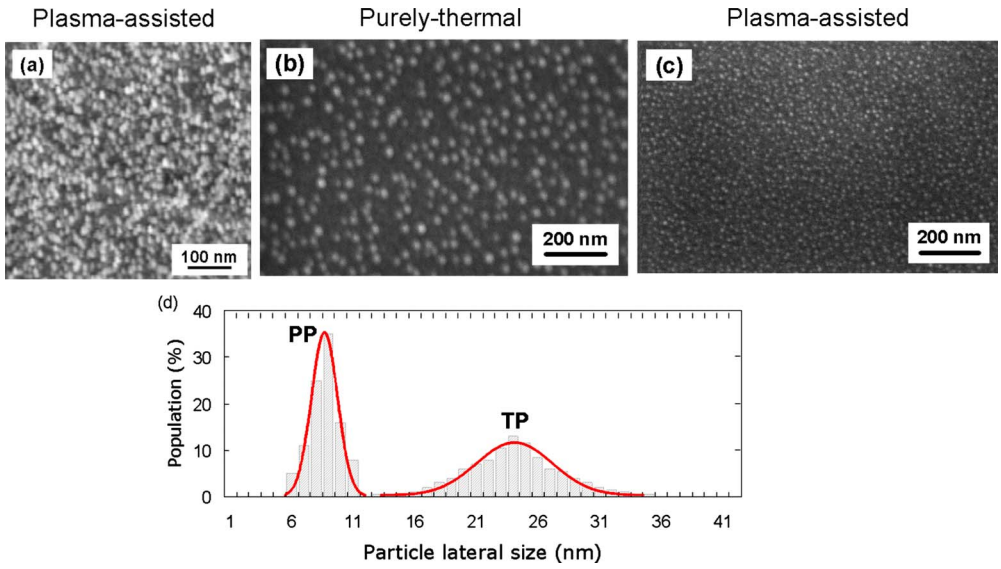

FIG. 2. (Color online) (a) AFM analysis of 1 nm Fe deposited onto TiN and pretreated for 5 min at 550 °C under PP in 100 mbar of H_2 and a dc plasma power of 50 W (500×500 nm^2). [(b) and (c)] SEM images of 1 nm Fe deposited onto TiN and pretreated by TP and PP, respectively, at 600 °C. (d) Histograms showing lateral size distribution with Gaussian fitting (red solid lines) of nanoparticles obtained in (b) and (c).

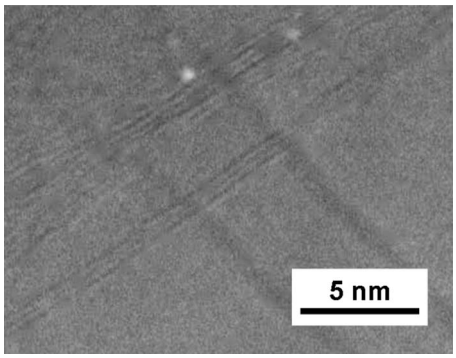

FIG. 4. HRTEM of CNTs grown on TiN/Fe films receiving PP. Growth conditions are 600 °C for 10 min in 0.5 mbar of C_2H_2. CNTs have parallel and continuous walls.

that observed using the Al_2O_3/Fe system.[11] There, alignment arises from the strong Fe–Al_2O_3 interaction, which inhibits the sintering of Fe nanoparticles. We thus suggest that PP promotes catalyst-support interactions, which stabilize smaller size catalyst particles. This is consistent with the observed base growth. Figures 5(b) and 5(d) schematically illustrate CNT growth for TP and PP films.

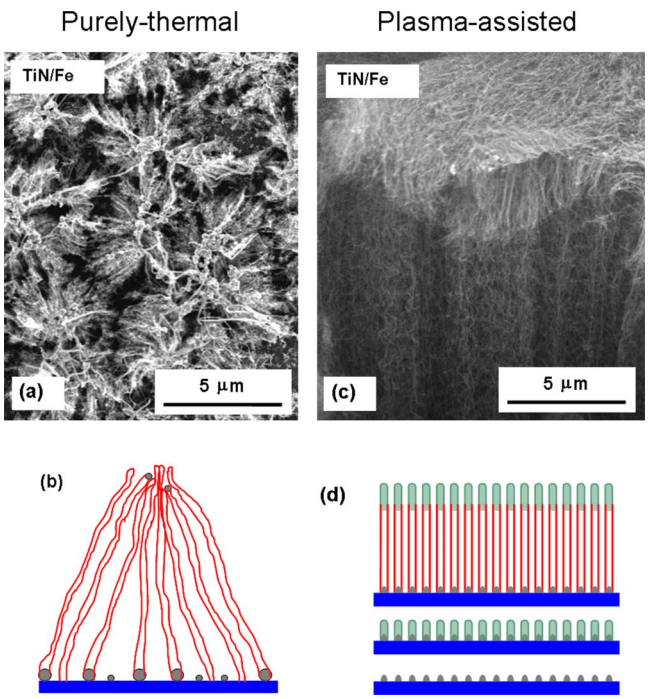

FIG. 5. (Color online) SEM images of CNTs grown for 10 min in 0.5 mbar of C_2H_2 at 600 °C on ~1 nm Fe with (a) TP and (c) PP, with supply of hydrocarbon for ~1 min, stopped for 5 min, and restarted for another 5 min. (b) and (d) are schematics of the growth processes for TP and PP, respectively.

In summary, we have demonstrated that Ni, Co, or Fe nanoparticles obtained by PP create high-density mats of small-diameter CNTs on conductive TiN supports. The key role of the plasma is to enhance the catalyst-support interaction, inhibiting sintering and reducing both the catalyst particle size and size distribution. The nanoparticles promote the growth of VACNTs with a high degree of homogeneity over large areas. PP may find applications in microelectronics, since it provides a useful path to large scale growth of VACNTs.

We acknowledge help from C. Zhang and F. Yan. This work was funded by VIACARBON Project No. ICT-2007 8.1-216668. S.H. acknowledges funding from the Royal Society.

[1] P. Avouris and J. Chen, Mater. Today **9**, 46 (2006).
[2] S. Fan, M. G. Chapline, N. R. Franklin, T. W. Tombler, A. M. Cassell, and H. Dai, Science **283**, 512 (1999).
[3] M. Katagiri, N. Sakuma, M. Suzuki, T. Sakai, S. Sato, T. Hyakushima, M. Nihei, and Y. Awano, Jpn. J. Appl. Phys. **47**, 2024 (2008).
[4] M. Nihei, M. Horibe, A. Kawabata, and Y. Awano, Jpn. J. Appl. Phys. **43**, 1856 (2004).
[5] J. Robertson, G. Zhong, H. Telg, C. Thomsen, J. M. Warner, G. A. D. Briggs, U. Detlaff, and S. Roth, Appl. Phys. Lett. **93**, 163111 (2008).
[6] X. Li, A. Cuo, Y. J. Jung, R. Vajtai, and P. M. Ajayan, Nano Lett. **5**, 1997 (2005).
[7] C. Bower, W. Zhu, S. Jin, and O. Zhou, Appl. Phys. Lett. **77**, 830 (2000).
[8] K. B. K. Teo, S. B. Lee, M. Chhowalla, V. Semet, V. T. Binh, A. Loiseau, G. Amaratunga, and W. I. Milne, Nanotechnology **14**, 204 (2003).
[9] M. Pinault, V. Pichot, H. Khodja, P. Launois, C. Reynaud, and M. Mayne-L'Hermite, Nano Lett. **5**, 2394 (2005).
[10] T. Iwasaki, R. Morikane, T. Edura, M. Tokuda, K. Tsutsui, Y. Wada, and H. Kawarada, Carbon **45**, 2351 (2007).
[11] C. Mattevi, C. T. Wirth, S. Hofmann, R. Blume, M. Cantoro, C. Ducati, C. Cepek, A. Knop-Gericke, S. Milne, C. Castellarin-Cudia, S. Dolafi, A. Goldoni, R. Schloegl, and J. Robertson, J. Phys. Chem. C **112**, 12207 (2008).
[12] A. M. Rao, D. Jacques, R. C. Haddon, W. Zhu, C. Bower, and S. Jin, Appl. Phys. Lett. **76**, 3813 (2000).
[13] T. de los Arcos, F. Vonau, M. G. Garnier, V. Thommen, H.-G. Boyen, P. Oelhafen, M. Duggelin, D. Mathis, and R. Guggenheim, Appl. Phys. Lett. **80**, 2383 (2002).
[14] Y. Wang, Z. Luo, B. Li, P. Ho, Z. Yao, L. Shi, E. N. Bryan, and R. J. Nemanich, J. Appl. Phys. **101**, 124310 (2007).
[15] D. Yokoyama, T. Iwasaki, T. Yoshida, H. Kawarada, S. Sato, T. Hyakushima, M. Nihei, and Y. Awano, Appl. Phys. Lett. **91**, 263101 (2007).
[16] J. García-Céspedes, S. Thomasson, K. B. K. Teo, I. A. Kinloch, W. I. Milne, E. Pascual, and E. Bertran, Carbon **47**, 613 (2009).
[17] Q. Fu and T. Wagner, Surf. Sci. Rep. **62**, 431 (2007).
[18] S. Hofmann, M. Cantoro, B. Kleinsorge, C. Casiraghi, A. Parvez, J. Robertson, and C. Ducati, J. Appl. Phys. **98**, 034308 (2005).
[19] M. Cantoro, S. Hofmann, C. Mattevi, S. Pisana, A. Parzev, A. Fasoli, C. Ducati, V. Scardaci, A. C. Ferrari, and J. Robertson, J. Appl. Phys. **105**, 064304 (2009).